ARTICLE IN PRESS

BBAPAP-39508; No. of pages: 9; 4C: 6, 8

Biochimica et Biophysica Acta xxx (2015) xxx–xxx

Contents lists available at ScienceDirect

Biochimica et Biophysica Acta

journal homepage: www.elsevier.com/locate/bbapap

Functional roles of the hexamer organization of plant glutamate decarboxylase ☆

Alessandra Astegno [a,*], Guido Capitani [b], Paola Dominici [a]

[a] Department of Biotechnology, University of Verona, Strada Le Grazie 15, Verona (VR), Italy
[b] Paul Scherrer Institut, Villigen 5232, Switzerland

ARTICLE INFO

Article history:
Received 12 November 2014
Received in revised form 30 December 2014
Accepted 7 January 2015
Available online xxxx

Keywords:
Glutamate decarboxylase
Dimer–hexamer equilibrium
N-terminal domain
Calmodulin

ABSTRACT

Glutamate decarboxylase (GAD) is a pyridoxal 5′-phosphate (PLP)-dependent enzyme that catalyzes the α-decarboxylation of glutamate to γ-aminobutyrate. A unique feature of plant GAD is the presence of a calmodulin (CaM)-binding domain at its C-terminus. In plants, transient elevation of cytosolic Ca^{2+} in response to different types of stress is responsible for GAD activation via CaM. The crystal structure of GAD isoform 1 from *Arabidopsis thaliana* (AtGAD1) shows that the enzyme is a hexamer composed of a trimer of dimers. Herein, we show that in solution AtGAD1 is in a dimer–hexamer equilibrium and estimate the dissociation constant (K_d) for the hexamer under different conditions. The association of dimers into hexamers is promoted by several conditions, including high protein concentrations and low pH. Notably, binding of Ca^{2+}/CaM1 abolishes the dissociation of the AtGAD1 oligomer. The AtGAD1 N-terminal domain is critical for maintaining the oligomeric state as removal of the first 24 N-terminal residues dramatically affects oligomerization by producing a dimeric enzyme. The deleted mutant retains decarboxylase activity, highlighting the dimeric nature of the basic structural unit of AtGAD1. Site-directed mutagenesis identified Arg24 in the N-terminal domain as a key residue since its mutation to Ala prevents hexamer formation in solution. Both dimeric mutant enzymes form a stable hexamer in the presence of Ca^{2+}/CaM1. Our data clearly reveal that the oligomeric state of AtGAD1 is highly responsive to a number of experimental parameters and may have functional relevance *in vivo* in the light of the biphasic regulation of AtGAD1 activity by pH and Ca^{2+}/CaM1 in plant cells. This article is part of a special issue titled "Cofactor-Dependent Proteins: Evolution, Chemical Diversity and Bio-applications."

1. Introduction

GAD (glutamate decarboxylase, EC 4.1.1.15) is a pyridoxal 5′-phosphate (PLP)-dependent enzyme that catalyzes the irreversible α-decarboxylation of L-glutamic acid to γ-aminobutyric acid (GABA) and carbon dioxide, which is the final step of the GABA shunt. GAD and GABA are present in virtually all organisms but exhibit different regulatory mechanisms and biological functions. They are involved in resistance to cytosolic acidosis in bacteria [1], whereas GABA is an important inhibitory neurotransmitter in animals [2,3]. The role of GABA in plants remains unclear. In addition to the well-documented roles of GABA as a buffering mechanism in C and N metabolism and in regulation of cytosolic pH [4], it has a significant role in protection against oxidative stress [5] and defense against herbivorous pests [6]. In this regard, because of the rapid increases in GABA concentration in response to stress, it has sometimes been inferred that GABA might act as an intracellular signaling molecule in plants [7–9].

Compared to GADs from other organisms, plant GADs possess a unique feature, namely, the presence of a C-terminal calmodulin binding site (CaMBD). This characteristic confers plant GADs an additional regulatory mechanism by making them responsive to cytosolic calcium (Ca^{2+}), thus revealing that at least two mechanisms exist, by which GAD activity can be stimulated *in vitro* and *in vivo*, namely, acidic pH and Ca^{2+}/CaM [10–12].

The sequence of the completed *Arabidopsis* genome indicates that five isoforms of GAD exist in *A. thaliana* (AtGAD1-AtGAD5) [13]. Isoform 1 (AtGAD1) was recently characterized both biochemically and structurally by Gut et al. [14]. The crystal structure revealed that the enzyme belongs to the fold Type I family of PLP-enzymes and is a compact homohexamer of 342 kDa similar to the bacterial enzyme GadB [15].

Abbreviations: GAD, Glutamate decarboxylase; CaM1, calmodulin isoform 1 from *Arabidopsis thaliana*; GABA, γ-aminobutyric acid; PLP, pyridoxal 5′-phosphate; PDB, Protein Data Bank; K_d, dissociation constant; SEC, size exclusion chromatography; FPLC, fast protein liquid chromatography; PAGE, polyacrylamide gel electrophoresis; DTT, dithiothreitol; SAXS, small-angle X-ray scattering; CaMBD, calmodulin binding domain; T_{50}, thermal inactivation midpoint.

☆ This article is part of a Special Issue titled Cofactor-Dependent Proteins: Evolution, Chemical Diversity and Bio-applications.

* Corresponding author at: Alessandra Astegno, Department of Biotechnology, University of Verona, Strada Le Grazie 15, Verona (VR), Italy. Tel.: +39 045 8027955; fax: +39 045 8027929.
E-mail address: alessandra.astegno@univr.it (A. Astegno).

http://dx.doi.org/10.1016/j.bbapap.2015.01.001
1570-9639/

The hexamer is a trimer of dimers, consisting of two layers of three subunits each, where the dimers contribute one subunit to each layer (PDB ID: 3HBX) (Fig. 1). Each subunit can be divided into an N-terminal domain (residues 1–57), a large domain (residues 58–347) containing the cofactor binding site, a small domain (residues 348–448), and a C-terminal domain containing a CaMBD that regulates enzyme activity in a CaM-dependent manner.

A low-resolution structure of the AtGAD1 in complex with the calmodulin isoform 1 (CaM1) from *Arabidopsis thaliana* obtained by small-angle X-ray scattering (SAXS) showed that CaM1 activates AtGAD1 by relieving two C-terminal autoinhibition domains of adjacent active sites, thereby forming a 393 kDa AtGAD1-Ca^{2+}/CaM1 complex with an unusual 1:3 stoichiometry. In the complex, one CaM1 molecule attaches to two AtGAD1-CaMBDs of neighboring subunits in the homohexameric enzyme, activating two adjacent active sites by relief of the corresponding autoinhibitory domains [14].

While PLP-enzymes have been extensively investigated, less is known about their quaternary structures in solution and the dynamics of subunit dissociation/association. Herein, we analyze the essential factors governing the stability of AtGAD1 quaternary structure. We show that the oligomeric state of AtGAD1 depends on concentration, revealing an equilibrium between two species in solution, a dimer and a hexamer. The association of dimers into hexamers is promoted by a number of conditions, including high enzyme concentration, presence of Ca^{2+}/CaM1, and acidic pH (pH < 6.5). Guided by sequence analysis of N-terminal domains of plant GADs, by the AtGAD1 crystal structure, and by limited tryptic proteolysis, we have identified a flexible and exposed stretch spanning residues 1–24 as the minimal region required for assembly and stabilization of the hexameric state. This was achieved using a combination of biochemical analyses on a purified recombinant protein where the first 24 N-terminal amino acids had been deleted (AtGAD1-Δ1-24). In addition, site-directed mutagenesis allowed for identification of a crucial hexamerization 'hot spot' in the N-terminal domain, Arg24, which forms a contact network between the dimeric units. Taken together, the results obtained *in vitro* support a model of biphasic regulation of AtGAD1 oligomerization and activity *in vivo*.

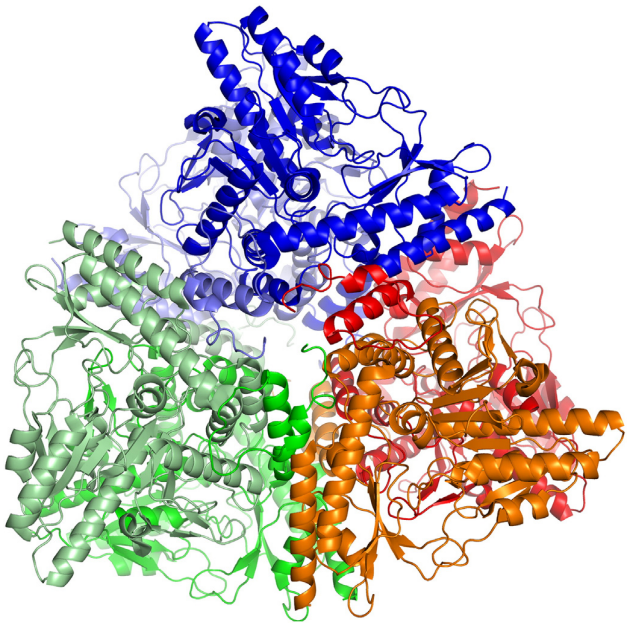

Fig. 1. Cartoon representation of AtGAD1. The six subunits are depicted in different colors. The three dimers are A–B (blue and light blue), C–D (red and orange), and E–F (green and light green) (PDB ID: 3HBX) [14].

2. Materials and methods

2.1. Cloning, expression, and purification of recombinant GAD1 mutants and CaM1

Construction of the N-terminally truncated AtGAD1 mutant AtGAD1-Δ1-24, where the first 24 residues of the mature polypeptide chain are absent, was performed by PCR amplification of the plasmid pET12b carrying the gene encoding AtGAD1. Two primers were used: the first annealed from the 25th codon and contained an additional upstream nucleotide sequence used to introduce an *Nde*I restriction site at the 5′-end, which provided the necessary ATG start codon (forward primer 5′-GCTCTAGACATATGACTTCACTTCCTAGG-3′; *Nde*I *site* is underlined), and the second primer annealed over the C-terminus of AtGAD1 (reverse primer 5′-CGGGATCCTTAGCAGATACCACTCG-3′; *Bam*HI is underlined).

The resulting DNA fragment was inserted into pET12b at the *Nde*I/*Bam*HI sites for directional cloning, replacing the wild-type gene to yield the construct pET12b-AtGAD1-Δ1-24. The newly generated plasmid pET12b-AtGAD1-Δ1-24 was fully sequenced to confirm the deletion and used to transform the *Escherichia coli* strain BL21(DE3)pLysS.

The N-terminal point mutants were made on the wild-type (wt) construct pET12b-AtGAD1 using the QuikChange™ site-directed mutagenesis kit (Stratagene, CA, USA) following the manufacturer's protocol. For each mutant, two synthetic oligonucleotide primers were designed (Invitrogen), each complementary to opposite strands of the plasmid and containing the desired mutation. The coding region of all mutated plasmids was verified by DNA sequencing. *E. coli* strain BL21(DE3)pLysS cells were transformed and used for expression.

The conditions for expression and purification of the mutants were essentially as described previously for AtGAD1 wt [14]. The PLP content of all preparations was determined by treating proteins with 0.1 M NaOH and measuring absorbance at 388 nm ($\varepsilon_{388} = 6550\ M^{-1}\ cm^{-1}$). Enzyme concentration was determined as described for the wt enzyme [14].

CaM1 from *A. thaliana* was expressed in *E. coli* strain BL21(DE3) containing plasmids encoding for CaM1 (pET12b-CaM1). The cell culture was grown to exponential phase in LB medium containing ampicillin (100 μg/mL) at 37 °C, and induction was done with 0.5 mM isopropyl-β-D-thiogalactopyranoside (IPTG) for 4–5 h at 30 °C. CaM1 was purified essentially as described by Liao and Zielinski [16]. Protein concentration was determined by the Bradford assay [17].

2.2. AtGAD1 activity assay

Enzyme assays were performed as described [18]. To test the effect of temperature on decarboxylase activity of wt and mutant proteins, a temperature profile was obtained. The protein (0.2 mg/mL) in an aqueous buffer containing 25 mM MES, 25 mM MOPS, and 150 mM NaCl at pH 5.8 was incubated for 15 min at temperatures between 30 °C and 90 °C. Samples were removed, cooled on ice for 3 min, and diluted to the concentrations used for assay of enzymatic activity. Residual enzymatic activity was determined as described above.

2.3. Spectroscopic measurements

Absorption measurements were carried out on a JASCO-V560 UV-Visible spectrophotometer. Absorbance data were recorded at 415 nm and at 338 nm in a solution containing 25 mM MES, 25 mM MOPS, and 150 mM NaCl and fitted to Eqs. (1) and (2), respectively:

$$A = \frac{(A_1 - A_2)}{(1 + 10^{(pH - pKa)})} + A_2 \quad (1)$$

$$A = \frac{(A_1 - A_2)}{(1 + 10^{(pKa - pH)})} + A_2 \quad (2)$$

Please cite this article as: A. Astegno, et al., Functional roles of the hexamer organization of plant glutamate decarboxylase, Biochim. Biophys. Acta (2015), http://dx.doi.org/10.1016/j.bbapap.2015.01.001

where A_1 and A_2 are the high and low absorbance limits at a particular wavelength, respectively [14].

2.4. Size exclusion chromatography

The effects of protein concentration, pH, and NaCl concentration on the oligomerization state of AtGAD1 wt and its mutants were monitored by analytical size exclusion chromatography (SEC) using an FPLC system (GE Healthcare) with a Superdex 200 HR 10/30 column (GE Healthcare). After 10 min incubation at room temperature, the protein was loaded into a 100 μL injection loop at a flow rate of 0.1 mL/min. All solutions used to study pH effects contained 50 mM HEPES, 150 mM NaCl, 0.1 mM DTT, and 0.5 mM $CaCl_2$. To study the influence of NaCl concentration, the same buffer containing NaCl from 0.15 to 0.8 M was used.

To determine the K_d, various amounts of AtGAD1 were used in the range of 0.083–30 μM (enzyme concentration expressed in hexamer equivalents).

Calibration of the Superdex 200 column was performed with high and low molecular mass gel filtration calibration kits (Sigma) according to the manufacturer's instructions.

The relative amount of each oligomer was measured by integration of the area under the curve (absorbance at 280 nm) using PeakFit™ software (Systat Software) designed to resolve overlapping peaks using Gaussian peak resolving method.

2.5. Evaluation of K_d values

$[H_{TOT}]$ denotes the maximal amount of AtGAD1 hexamer, $[H_{TOT}] = {}^{[D]}/_{3} + [H]$, where $[H]$ and $[D]$ denote the concentrations of hexameric and dimeric species, respectively. The hexamer dissociation constant, $K_d = [D]^3/[H]$, can be estimated as follows [19].

Given the following expression:

$$\%H = 100\frac{[H]}{[H_{TOT}]} \quad \text{and} \quad [D] = 3([H_{TOT}]-[H])$$

K_d can be expressed as follows:

$$K_d = \frac{3^3([H_{TOT}]-[H])^3}{[H]} = [H_{TOT}]^2\,\frac{0.0027(100-\%H)^3}{\%H}$$

By applying the logarithm, the following expression is obtained:

$$\log\underbrace{\left(\frac{\%H}{0.0027100-\%H^3}\right)}_{f\%H} = 2\cdot\log([H_{TOT}]) - \log(K_d)$$

Thus, a plot of $f(\%H)$ versus $\log([H_{TOT}])$ will yield a straight line with a slope of 2. When $f(\%H) = 0 \Rightarrow Kd = [H_{TOT}]^2$.

From this, the AtGAD1 concentration at equilibrium is obtained, i.e., the $[H_{TOT}]$ value when [D] = [H].

From the K_d definition ($K_d = [D]^3/[H]$), the following is obtained:

$$K_d = [D]^3/[H] = [D]^2 \quad \Rightarrow \quad \sqrt{K_d} = [D] = [H]$$

Thus, $[H_{TOT}]$ at equilibrium can be expressed as follows:

$$[H_{TOT}] = \frac{[D]}{3} + [H] = \frac{4}{3}\sqrt{K_d}$$

Therefore, when the hexamer-equivalent concentration is higher than $\frac{4}{3}\sqrt{K_d}$, the equilibrium will shift toward the hexamer, whereas when the hexamer-equivalent concentration is lower than $\frac{4}{3}\sqrt{K_d}$, the equilibrium will shift toward the dimer.

2.6. Native PAGE analysis

The oligomeric state of native AtGAD1 and its mutants was determined by Ferguson plots [20]. The protein (approximately 1 mg/mL) was electrophoresed through non-denaturing 7%, 8%, 9%, and 10% polyacrylamide gels. The retardation coefficient (K_r) was calculated by plotting 100 [log (R_f x 100)] against the acrylamide concentration (where R_f is relative mobility determined for each protein relative to the tracking dye) and determining the negative slope of this line. The log of the negative slope was plotted against the log of molecular mass to obtain a standard curve [20]. α-Lactalbumin (14 kDa), carbonic anhydrase (29 kDa), chicken egg albumin (45 kDa), and bovine serum albumin (monomer 66 kDa and dimer 132 kDa) were used as standards.

2.7. Limited proteolysis

Thirty micrograms of AtGAD1 was treated with trypsin (1:500 w/w) in 50 mM HEPES, pH 7.3 at 25 °C. At various time intervals, aliquots (4 μg AtGAD1) were removed for SDS–PAGE analyses. The digestion reaction was stopped by rapid addition of reducing sample buffer and boiling for 2 min. In order to isolate the proteolytic fragment, 250 μg of AtGAD1 were incubated with trypsin for 30 min. The reaction was stopped by adding a two-fold weight excess of soybean trypsin inhibitor and the proteolysis product was purified on a Superdex 200 HR 10/30 column.

3. Results

3.1. AtGAD1 exists in solution as a dimer–hexamer equilibrium

Size exclusion chromatography (SEC) was used to analyze the amount of dimer and hexamer present in protein samples. To minimize artifacts arising from the interaction between AtGAD1 and the column matrix, the addition of 0.15 M NaCl was required.

At physiological pH (pH 7.2), two characteristic peaks with elution volumes of about 11.2 and 13.3 mL were observed. The corresponding relative molecular masses, estimated from the elution volume of the standard proteins, were 340 kDa and 114 kDa, respectively, corresponding to approximately six and two monomer subunits (Fig. 2a). These masses reflect the theoretical calculated hexamer and dimer forms of AtGAD1. Thus, at physiological pH, AtGAD1 exists in two oligomeric forms, the hexamer and the dimer, and no other species are observed. When the fractions containing the hexamer were re-injected onto the same column, a substantial amount of dimer eluted, indicating that oligomerization of the dimer is reversible (data not shown).

Consistent results were obtained by native PAGE analysis. As shown in Fig. 2b, when AtGAD1 was analyzed by native PAGE two bands were observed, the relative mobilities of which decreased as the acrylamide concentration was increased from 7% to 10%. The retardation coefficient was calculated to be 19.21 and 10.86, respectively (Fig. 2c); these values correlate with estimated molecular masses of approximately 364 and 105 kDa, respectively, corresponding to hexameric and dimeric forms of AtGAD1.

The proportion of hexameric species increased as a function of the protein concentration. When SEC was performed over a range of AtGAD1 concentration from 0.083 to 30 μM (expressed in hexamer equivalents) at pH 7.2, the total areas under the elution peaks were proportional to the amounts of protein: while hexamer was predominant at high protein concentrations, dimer became the predominant species at low enzyme concentration.

The equilibrium constant for hexamer dissociation was determined according to the method of Manning [19] adapted to the hexamer–dimer equilibrium. A plot of percent hexameric AtGAD1 (%H) as a function of the total AtGAD1 concentration $[H_{TOT}]$ prior to application to the column yielded a hyperbolic-like curve. A representative dissociation curve for AtGAD1 is presented in Fig. 2d.

Please cite this article as: A. Astegno, et al., Functional roles of the hexamer organization of plant glutamate decarboxylase, Biochim. Biophys. Acta (2015), http://dx.doi.org/10.1016/j.bbapap.2015.01.001

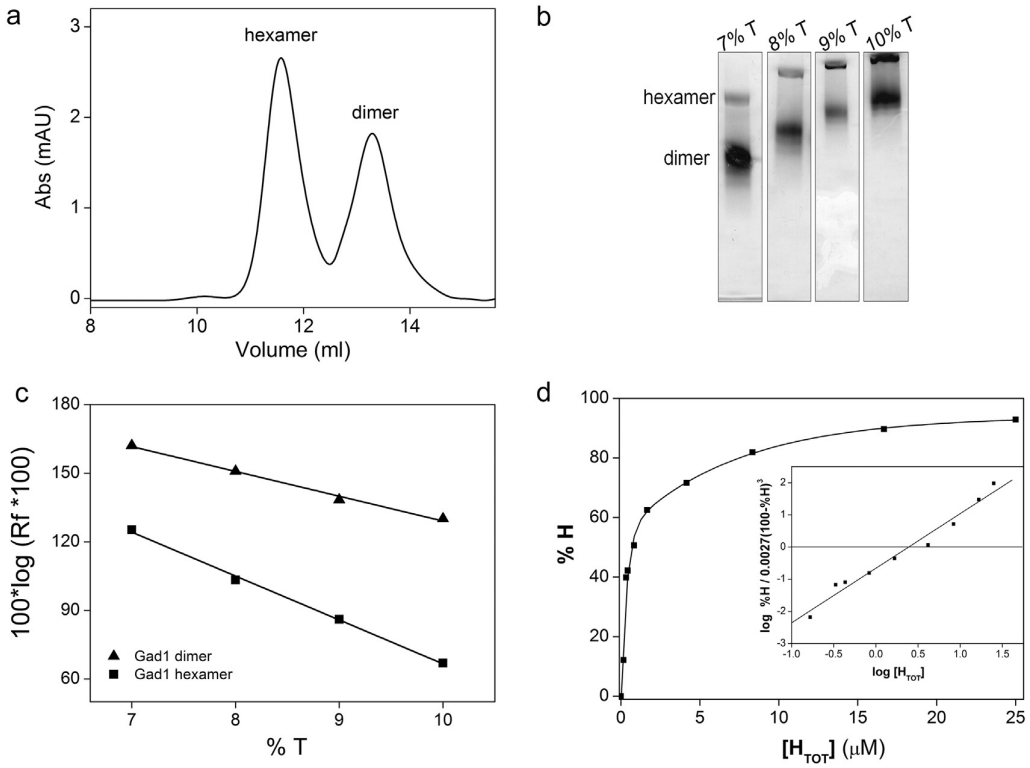

Fig. 2. Oligomerization state of AtGAD1. (a) SEC of 0.43 μM $AtGAD1_{hex}$ (expressed as hexamer equivalents) in 50 mM HEPES, 150 mM NaCl, and 0.1 mM DTT at pH 7.2. (b) Native PAGE of AtGAD1 at 7%T, 8%T, 9%T, and 10%T. (c) Effect of %T on the relative mobility of AtGAD1. Plot according to Ferguson et al. [20] of 100 [log ($R_f \times 100$)] *versus* %T. The slope of such a plot is referred to as the retardation coefficient (K_r). (d) Representative dissociation curve of protein concentration effects on AtGAD1 hexamer dissociation at pH 7.2 in 50 mM HEPES, 150 mM NaCl, and 0.1 mM DTT. [H_{TOT}] represents the concentration of hexamer that would be present if the protein was all hexamer, and % H represents the percentage of protein that is actually hexamer at various AtGAD1 concentrations. *Inset*: Plot according to Manning et al. [19].

A good fit to a slope of 2.0 was obtained, and the K_d value was calculated. At physiological salt concentration and pH 7.2, the hexamer–dimer equilibrium was characterized by a K_d value of $0.22 \times 10^{-12} \pm 0.01$ M^2 (Table 1).

3.2. AtGAD1 forms a hexamer at acidic pH, whereas it exists mainly as a dimer at physiological pH

To investigate the effect of pH on the dissociation of hexameric AtGAD1, SEC was performed in the pH range 6.0–8.0. Measurements were carried out at a protein concentration of 0.43 μM (in terms of hexamer equivalents), at which the dissociation equilibrium can be easily studied across the pH interval. As the pH increased, the peak corresponding to the hexameric form decreased, while that corresponding to the dimer increased (Fig. 3a). The apparent molecular mass of AtGAD1 was plotted as a function of pH (not shown). The results indicated that AtGAD1 exists as a hexamer in the pH range of 6.0–7.0, while dimeric enzyme was predominant at pH 7.0–8.0. Hexameric AtGAD1 began to dissociate with a transition midpoint of pH 6.9, forming a dimeric enzyme as the major form at pH values higher than 7.0. The interconversion between the hexameric and the dimeric forms is not complete in this pH range. Attempts to measure the dimer–hexamer equilibrium at pH > 8 were unsuccessful since the resulting chromatograms showed evidence of peak broadening and inconsistencies in peak elution volumes.

To analyze dimer–hexamer interactions, SEC at various concentrations of AtGAD1 was used to determine dissociation constants as a function of NaCl concentration between 0.15 and 0.8 M. In general, an increase in salt concentration appeared to cause destabilization of the hexamer interaction, as demonstrated by the evidence that in the presence of 0.8 M NaCl, the hexamerization degree of AtGAD1 decreased to 60%.

Table 1
Effect of concentration at pH 7.2 on the percentage of AtGAD1 hexamer during SEC.[a]

Concentration (μM)[b]	% hexamer
0.084	30.24
0.17	39.31
0.34	45.07
0.44	46.76
0.84	59.67
1.67	71.66
4.167	82.39
8.34	90.36
16.67	93.6
25	100
33.34	100

[a] The elution was followed by absorbance at 280 nm and the amounts of protein present as hexamer were determined using the PeakFit program.
[b] Enzyme concentration is expressed in hexamer equivalents.

3.3. Binding of Ca^{2+}/CaM1 at the C-terminus of AtGAD1 induces hexamer formation at physiological pH

Binding of Ca^{2+}/CaM1 at C-terminus of AtGAD1 essentially abolishes both pH- and protein concentration-dependent AtGAD1 dissociation: in the presence of Ca^{2+}/CaM1 over the entire pH range probed and for each enzyme concentration, there was only one peak with an elution volume of ~10.8 mL, corresponding to a high molecular mass complex

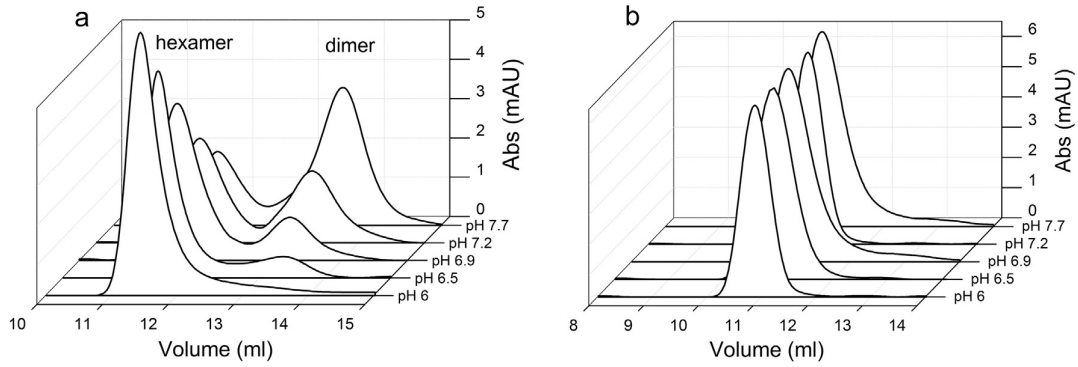

Fig. 3. AtGAD1 and AtGAD1-Ca^{2+}/CaM1 complex elution profiles at different pH values. (a) SEC profiles of dimeric and hexameric forms of 0.43 μM AtGAD1 recorded in 50 mM HEPES, 150 mM NaCl, and 0.1 mM DTT at pH 6, 6.5, 6.9, 7.2, and 7.7. (b) SEC profiles of AtGAD1 in the presence of Ca^{2+}/CaM1 recorded in 50 mM HEPES, 150 mM NaCl, 0.1 mM DTT, and 0.5 mM $CaCl_2$ at pH 6, 6.5, 6.9, 7.2, and 7.7.

of ~439 kDa (Fig. 3b) that is in agreement with the 1:3 AtGAD1-Ca^{2+}/CaM1 stoichiometry previously determined by SAXS.

3.4. The first 24 N-terminal residues of AtGAD1 are critical for hexamer formation

The 3D structure of AtGAD1 indicates that the N-terminal domain of each subunit is involved in hexamer formation and stabilization [14]. To elucidate the specific role of this domain on AtGAD1 dimer–hexamer equilibrium and to determine the region required for hexamer formation, we examined the oligomeric states of several N-terminus mutants.

Guided by sequence analysis of plant GADs N-terminus domains, by the crystal structure of AtGAD1 and by limited tryptic digestion (not shown), we identified a flexible and exposed stretch spanning residues 1–24 as the minimum region required for assembly of hexamer.

The mutant enzyme AtGAD1-Δ1-24 was analysed by SEC at pH values ranging from 6.0 to 8.0, and a striking difference with the wt protein emerged. Across the above pH range, AtGAD1-Δ1-24 eluted as a single peak, the position of which corresponded to a species with a molecular mass of ~110 kDa. Thus, the truncated enzyme exists as a dimer across the pH range and deleting the first 24 N-terminal amino acid had a dramatic effect on the oligomeric state of AtGAD1 (Fig. 4a). The peak

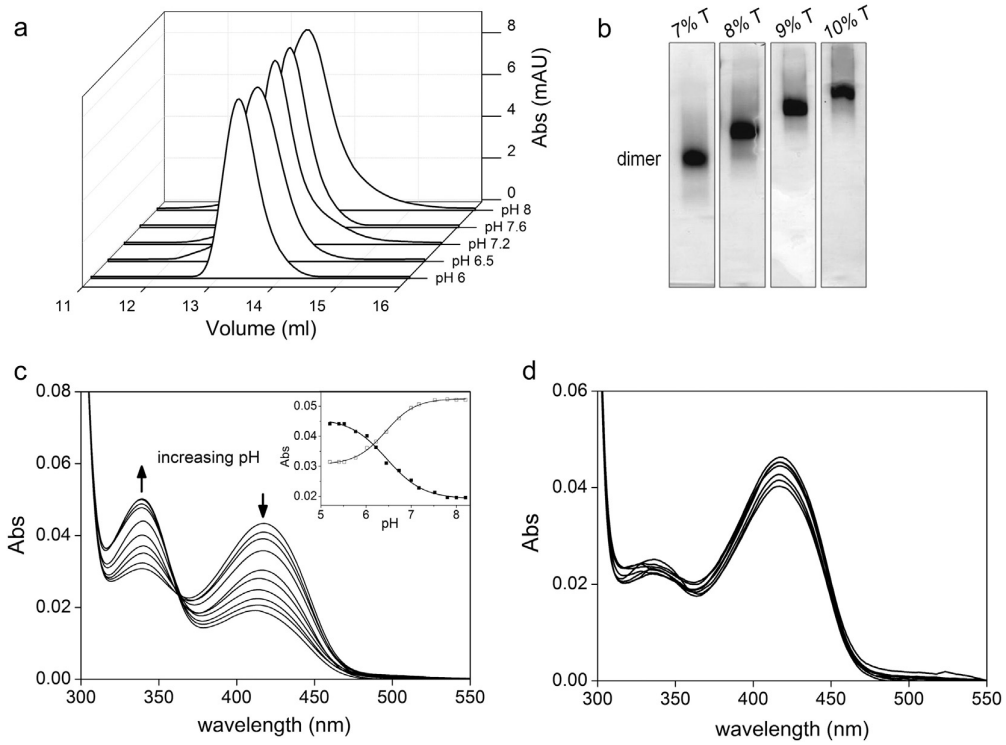

Fig. 4. Properties of AtGAD1-Δ1-24. (a) SEC profiles of 1.29 μM AtGAD1-Δ1-24 (enzyme concentration is expressed in dimer equivalents) recorded in 50 mM HEPES, 150 mM NaCl, and 0.1 mM DTT at pH 6, 6.5, 7.2, 7.6, and 8. (b) Native PAGE of AtGAD1-Δ1-24 at 7%T, 8%T, 9%T, and 10%T. (c) Absorbance spectra of 4 μM GAD1-Δ1-24 recorded in 25 mM MES, 25 mM MOPS, and 150 mM NaCl at pH 5.52, 5.77, 6.02, 6.22, 6.45, 6.73, 7.0, 7.17, 7.52, and 7.8. *Inset*: pH dependence of the absorbances at 338 nm (□) and at 415 nm (■). The solid lines represent the theoretical curves according the Eqs. (1) and (2): 415 nm ($pK_a = 6.43 \pm 0.02$, Eq. (1)) and 338 nm ($pK_a = 6.45 \pm 0.02$, Eq. (2)). (d) Absorbance spectra of 4 μM AtGAD1-Δ1-24-Ca^{2+}/CaM1 complex recorded at pH 5.52, 5.77, 6.02, 6.22, 6.45, 6.73, 7.0, 7.17, 7.52, and 7.8.

Please cite this article as: A. Astegno, et al., Functional roles of the hexamer organization of plant glutamate decarboxylase, Biochim. Biophys. Acta (2015), http://dx.doi.org/10.1016/j.bbapap.2015.01.001

profile of AtGAD1-Δ1-24 along the entire pH range is symmetric, highlighting that the dimer is the only oligomeric species in solution.

Native PAGE analysis of the mutant protein (Fig. 4b) provided results consistent with the SEC ones: AtGAD1-Δ1-24 migrated as a single band. Based on a retardation coefficient of 11.67, the molecular weight of the truncated enzyme was estimated to be ~120 kDa, which is consistent with a dimeric structure for the mutant.

Notably, binding of Ca^{2+}/CaM1 appears to restore the hexamer species, since the SEC profiles of the AtGAD1-Δ1-24-Ca^{2+}/CaM1 complex showed the same elution volume of the AtGAD1-Ca^{2+}/CaM1 complex across the entire pH range (data not shown) which is in agreement with a 1:3 stoichiometry for the AtGAD1 hexamer: CaM1 complex. This supports the hypothesis that CaM1 binding induces protein hexamerization, even in the absence of N-terminus domain.

Deletion of the N-terminus does not alter the spectroscopic properties of the enzyme. The AtGAD1-Δ1-24 mutant exhibits the same characteristic absorption bands of the wt enzyme, with maxima at 415 and 338 nm, which were attributed to the ketoenamine and enolimine forms of the Schiff base, respectively [14]. As for the wt enzyme, the relative intensities of the absorbances at 415 and 338 nm of the mutant are pH dependent: the 338 nm band increases with increasing pH, while the 415 nm band decreases. When absorption values at 338 nm and 415 nm were plotted against pH, a single ionization constant was found with a pK_a value of 6.45 ± 0.02 (Fig. 4c).

This spectral data indicated that the absence of the 24 N-terminal residues in the mutant protein did not compromise the pH dependence of the internal aldimine tautomeric equilibrium. Moreover, as for the wt enzyme, spectra of AtGAD1-Δ1-24 in the presence of Ca^{2+}/CaM1 are characterized by a lack of interconversion of the two tautomers, thus confirming the role of the C-terminal CaM binding region in regulating the spectral equilibrium (Fig. 4d).

In order to assess whether the deletion of the first 24 residues causes any change in enzyme activity, we tested the AtGAD1-Δ1-24 ability to perform decarboxylation. The pH dependence of the activity of AtGAD1 exhibits a bell-shaped profile, with maximum activity at pH 5.8 [14]. The activity profile of the mutant, which is dimeric across the entire pH range, is also pH dependent, suggesting that the N-terminal region does not contain residues involved in catalysis. At the optimal pH AtGAD1-Δ1-24 mutant had about 80% activity compared to the wt protein (Fig. 5a). At this pH, the activities of both AtGAD1 and AtGAD1-Δ1-24 were only marginally stimulated by Ca^{2+}/CaM1. However, differences between the native and truncated enzyme were observed in the basic limb. Mutant enzymatic activity decreased sharply with increasing pH: at pH 6.8, it was 23% of that of the wt enzyme at the same pH. Interestingly, in the physiological pH range, binding of CaM1 to AtGAD1-Δ1-24 causes greater activation than that seen in the wt enzyme and restores an activity profile similar to that of the AtGAD1-Ca^{2+}/CaM1 complex. This is likely related to CaM1-induced hexamerization of AtGAD1-Δ1-24, as observed in the SEC profiles.

The AtGAD1-Δ1-24 enzyme showed decreased thermal stability compared with the wt form. T_{50} values for the wt and mutant AtGAD1 decreased from 70 °C to 56 °C (Fig. 5b), suggesting that hexamerization strongly contributes to the stability of the enzyme.

3.5. Identification of key residue for hexamerization in the AtGAD1 N-terminal domain

The pH- and salt-dependent hexamer dissociation suggests that electrostatic interactions of residues at subunit interfaces play a pivotal role. Site-directed mutagenesis was used to identify residue(s) important for hexamerization.

Plant GADs possess four conserved basic residues in their first 24 N-terminal amino acid region (H5, H15, R21, and R24 in AtGAD1) (Fig. 6a). Two of the four residues (H15 and R24) are located at the interfaces between dimeric units.

To obtain insight into the importance of these salt bridges for hexamer assembly, single, double, triple, and quadruple mutations of the above four residues (mutated to Ala) were constructed in various combinations.

Characterization of the variants allowed for identification of R24 as a key residue for hexamerization. SEC profiles showed that AtGAD1-R24A eluted across the entire pH range as a single peak, the position of which corresponds to a dimeric species (data not shown), indicating that single replacement of Arg24 to Ala disrupts the hexamer. SEC experiments were also validated by native PAGE analysis (Fig. 6b), which showed that the electrophoretic pattern of the mutant is characterized by a dimeric band, as is the case for the Δ1-24 mutant. AtGAD1-R24A displayed no differences from GAD1-Δ1-24 in the pH dependence of UV-Vis spectra and in Ca^{2+}/CaM1 binding properties (data not shown).

4. Discussion

The *A. thaliana* GAD1 structure determined at 2.65 Å resolution (PDB ID: 3HBX) revealed that the enzyme assembles as a hexamer composed as a trimer of dimers [14]. An analysis of the intradimer versus interdimer interfaces in 3HBX using EPPIC [21] shows the former are much larger than the latter, with areas of ~5200 A^2 versus ~2100 A^2. The intradimer interfaces also possess many more core residues (52–53 versus 12) than the interdimer ones (details can be found at http://www.eppic-web.org/ewui/#id/3hbx).

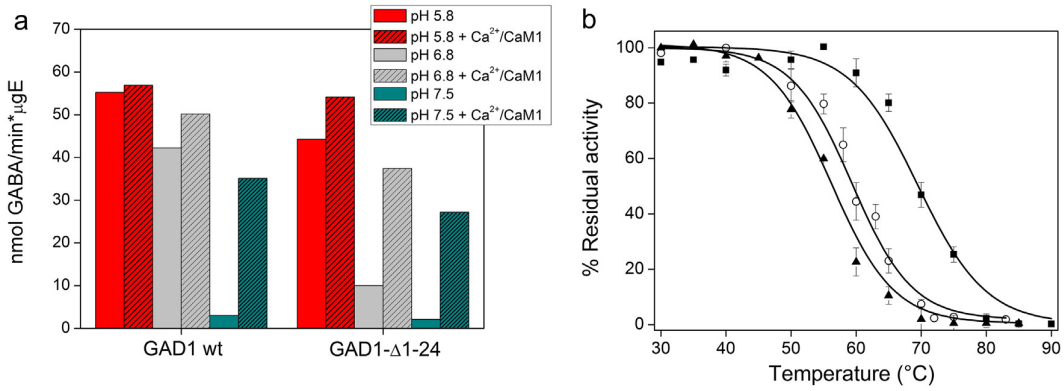

Fig. 5. Effects of N-terminus mutation on AtGAD1 catalytic activity and thermal stability. (a) Impact of pH and Ca^{2+}/CaM1 on the specific activity of AtGAD1 and AtGAD1-Δ1-24 mutant. Enzyme concentration for each assay was 0.6 μg. (b) Thermal stability profile of AtGAD1 wt (■), AtGAD1-Δ1-24 mutant, (▲) and AtGAD1-R24A (○). Residual activity was measured as described in the Section 2.2 after 15-min incubations at temperatures ranging between 30 °C and 90 °C. All activity assays were performed in a solution containing 25 mM MES, 25 mM MOPS, and 150 mM NaCl.

Please cite this article as: A. Astegno, et al., Functional roles of the hexamer organization of plant glutamate decarboxylase, Biochim. Biophys. Acta (2015), http://dx.doi.org/10.1016/j.bbapap.2015.01.001

Fig. 6. (a) Multiple sequence alignment of N-termini of plant GADs. The residues of the AtGAD1 N-terminal region subjected to mutational studies are indicated in bold. (b) Oligomerization state of AtGAD1-R24A; 7% native PAGE analysis of AtGAD1-R24A.

The results presented herein demonstrate that in solution AtGAD1 exists in an equilibrium of dimers and hexamers. The association of dimers into hexamers is promoted by several conditions, including high concentrations of the enzyme itself, the presence of Ca^{2+}/CaM1, and acidic pH (pH < 6.5). AtGAD1 dimers are prevalent at alkaline pHs. A decrease in pH to acidic values primes the association of dimers to hexamer such that oligomerization is complete at pH 6.0, which is the optimum pH of AtGAD1 catalytic activity. Association of dimers into hexamers is also affected by salt concentration, which favors hexamer dissociation.

If a hexamer reversibly dissociates, increases in the overall protein concentration should result in a higher hexamer–dimer ratio. Analyses of various concentrations of AtGAD1 by SEC and a plot of the results by Manning method [19] support this hypothesis and yield a K_d value at pH 7.2 of 0.22 μM^2 for a total concentration at equilibrium of 0.62 μM ($\frac{4}{3}\sqrt{K_d}$). Dilution of protein samples below this concentration would result in an equilibrium shift toward the dimeric form, while at concentrations higher than 0.62 μM the equilibrium is shifted toward the hexamer. This behavior could represent an effective mechanism for sensing protein concentration at physiological pH (see below).

Proton concentration appears to have a large influence on the dimer–hexamer equilibrium, since we found that the dimer–hexamer equilibrium is pH-dependent, with an increase in K_d values at alkaline pHs. The most significant changes in K_d occur in the pH range between 6.8 and 7.2, suggesting deprotonation of a residue(s) with a pK_a value of ~7.0. However, it is worth noting that a fraction of hexamer is still present at the more alkaline pH values we tested, thus indicating that the interactions between dimers are relatively stable.

Interestingly, Ca^{2+}/CaM1-binding essentially abolishes both pH and protein concentration-dependent AtGAD1 dissociation; in the presence of Ca^{2+}/CaM1 over the entire experimentally probed pH range and for every enzyme concentration, there was only one peak corresponding to a complex in which three CaM1s bind to a AtGAD1 hexamer.

The effects of salt on the hexamer interaction were consistent with the mostly polar nature of the dimer–dimer interface [14] and with the notion that electrostatic interactions contribute to hexamerization of AtGAD1. Electrostatic complementarity has been proposed to play a significant role in the formation of a large number of protein complexes [22–24]. The shift in equilibrium toward AtGAD1 dimers at high salt concentrations is likely to be a result of charge shielding by the addition of ions and a reduction in the productive charge interactions.

The crystal structure of AtGAD1 indicates that the N-terminal domain (residues 1–57) plays an important role in the formation and stabilization of the dimer and hexamer [14]. We have identified the first 24 residues as the minimal region required for assembly of the hexamer.

Across the entire pH range and at every enzyme concentration tested, the truncated enzyme AtGAD1-Δ1-24 existed as a dimer highlighting the importance of the N-terminal region as a trigger for oligomerization (Fig. 4a). Deletion of the N-terminus does not alter the spectroscopic properties of the enzyme. Binding of Ca^{2+}/CaM1 appears to restore the hexamer species, since the SEC profiles of AtGAD1-Δ1-24-Ca^{2+}/CaM1 complex showed the same elution volume of the AtGAD1-Ca^{2+}/CaM1 complex across the entire pH range.

Of note, the dimeric AtGAD1-Δ1-24 mutant maintains decarboxylase activity although it shows strongly reduced activity at physiological pH (i.e., approx. 4-fold decrease at pH 7). Therefore, the process of dissociation/reassociation might represent a potential control mechanism of catalytic activity since the dimeric form is less active than the hexameric one at physiological pH. Interestingly, in the physiological pH range, CaM1 binding to AtGAD1-Δ1-24 restores an activity profile similar to that of the AtGAD1-Ca^{2+}/CaM1 complex.

Mutagenesis analysis identified of a key residue in N-terminal domain, Arg24, which appears to be crucial in hexamer stabilization by forming a contact network between the dimeric units. Replacing Arg24 with Ala resulted in a mutant that was found exclusively in dimeric form as determined by SEC and native PAGE (Fig. 6b). The R24A enzyme was no different from AtGAD1-Δ1-24 in its pH dependence of UV-Vis spectra, catalytic activity, and Ca^{2+}/CaM binding properties.

In the three-dimensional structure of AtGAD1, the dimeric units are composed of subunits A and B, C and D, E and F. The hexamer interactions are between A and F, B and C, D and E. In particular, Arg24 from a subunit in one dimeric unit could be engaged in a salt bridge with Glu345 and Glu349 from a subunit of another dimeric unit; i.e., two residues from chain F, Glu345 and Glu349, are well positioned to form electrostatic interactions with Arg24 from chain A, thus strengthening interdimer interactions (Fig. 7). Since the structure was obtained from crystals grown in a high-salt condition, it is likely that the side chain orientations at physiological ionic strength are different from those observed in 3HBX; for instance, the side chain guanidinium moiety of Arg24 (A) could form a doubly hydrogen-bonded salt bridge with the side chain carboxylate of Glu349 (F) or with that of Glu345 (F).

The mutants AtGAD1-Δ1-24 and R24A, which are always dimeric in the absence of CaM1, behave as the wt enzyme in the presence of CaM1, indicating that CaM1 is able to induce hexamer formation by binding to two CaM1-binding domains of neighboring subunits.

The structure of AtGAD1 is similar to that of the bacterial enzyme GadB, and the two enzymes share the same fold and oligomeric assembly [14]. However, the key functional modules at the N- and C-termini of AtGAD1 and GadB differ significantly, reflecting local adaptation to different function/regulation. GadB becomes activated and recruited to the membrane at acidic pH [15]. This has been linked to a conformational change in the structure of the GadB N-terminal chain [25] from a flexible loop at pH 7.6 to a helix at acidic pH 4.6. In the GadB hexamer, this helix forms a triple helix bundle that is involved in the recruitment of GadB to the membrane when the cellular pH decreases. In contrast, the N-terminus of the AtGAD1 hexamer, which is also involved in the stabilization of hexameric structure by connecting the two layers of subunits,

Please cite this article as: A. Astegno, et al., Functional roles of the hexamer organization of plant glutamate decarboxylase, Biochim. Biophys. Acta (2015), http://dx.doi.org/10.1016/j.bbapap.2015.01.001

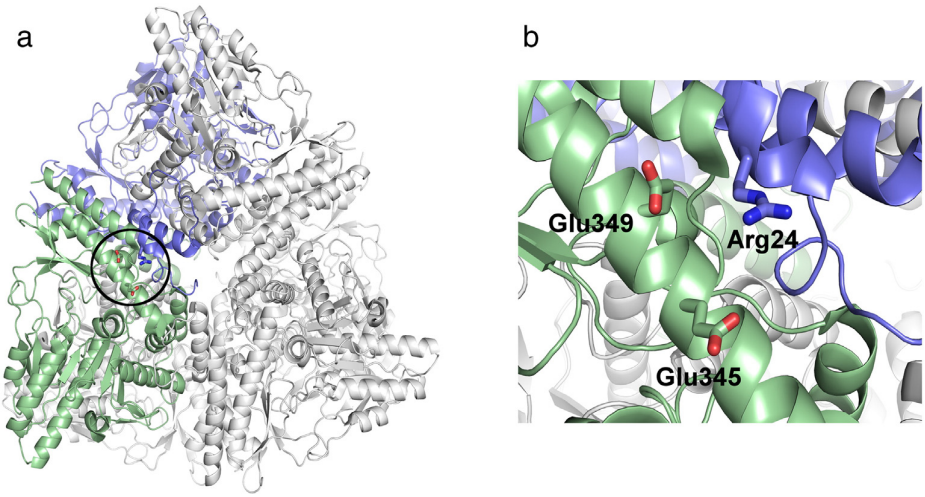

Fig. 7. (a) Structure of AtGAD1. Chain A of the protein is depicted in blue and chain F in green. (b) Close-up view of the environment of Arg24 (chain A, in blue) and Glu345 and Glu349 (chain F, in green) in the crystal structure of AtGAD1.

it cannot form such a bundle due to a small number of amino acid changes. Moreover, the C-terminal domain is remarkably different in GadB and AtGAD1. GadB uses an ~14 residue extension to regulate enzyme activity in a pH-dependent mode, while AtGAD1 possesses a CaM1-binding domain, which regulates enzyme activity in a CaM-dependent manner.

It appears that the regulatory mechanism of plant GAD is more complex than that of bacterial GAD. It is possible that *in vivo* AtGAD1 exists in oligomeric states other than the well-characterized X-ray diffraction hexameric state, which may be related to the high protein concentration and acidic pH used for protein crystallization. It should be questioned whether *in vitro* observations of different oligomer states are directly relevant for *in vivo* conditions. In plant cells, the local concentration of GAD is expectedly lower than those applied in the *in vitro* measurements, and thus caution should be used before directly inferring *in vivo* relevance to the oligomeric species. However, it is tempting to suggest that the qualitatively consistent observations from all applied methods, clearly revealing that AtGAD1 oligomeric state is highly responsive to a number of experimental parameters (protein concentration, pH, presence/absence of Ca^{2+}/CaM1, presence/absence of N-terminal), has some functional relevance, even *in vivo*. It seems plausible that regulation of AtGAD1 activity involves changes in the oligomeric state in response to *in vivo* conditions [10,26]. In plants under some conditions of stress (drought, temperature stress, salinity, or mechanical handling), GAD activity has been linked to increases in cytosolic Ca^{2+} concentrations [27], whereas in other stress conditions (exposure to high CO_2, hypoxia, and wounding), elevated GAD activity has been associated with decreases in pH [27,28]. Results from several investigations support a model for the *in vivo* biphasic stimulation of GAD and control of GABA accumulation in plants exposed to a variety of environmental stresses [10]. We thus suggest that our observations of responsive changes in the oligomeric state reflect one of the *in vivo* regulation(s) of AtGAD1 enzymatic activity (Scheme 1).

The concentration-dependent oligomerization properties of AtGAD1 could take part in a regulative mechanism to maintain the protein in a hexameric state under stress conditions. In particular, increased synthesis of AtGAD1 upon stress could fulfill the need of maintaining a constant supply of more active AtGAD1 hexamers, which would otherwise favor a shift in the oligomerization equilibria toward dissociation into less active dimers. A similar situation could be present when considering pH. Release of Ca^{2+} ions, however, would induce Ca^{2+}/CaM1 binding to AtGAD1, stabilizing the hexameric form (Scheme 1). Thus, CaM1 binding is supposed to exert an effect similar to low pH in keeping the protein in the more active hexameric form in response to stress conditions. Whereas the N-terminal domain of AtGAD1 triggers hexamerization and a subsequent increase in catalytic activity in response to acidic pH, the C-terminal domain triggers hexamerization through CaM binding to give a more active enzyme when cytosolic Ca^{2+} concentrations increase at physiological pH.

Our data clearly reveal that the oligomeric state of AtGAD1 is highly responsive to a number of experimental parameters and may have functional relevance *in vivo* in the light of the biphasic regulation of AtGAD1 activity by pH and Ca^{2+}/CaM1 in plant cells. It appears, therefore, that the coexistence of two levels of regulation of plant GAD is dictated by the need to respond flexibly to different kinds of cellular stress at different pH values and that plant GAD might respond quantitatively to its regulator.

Taken together, these data allow us to better understand the structural properties of AtGAD1 protein in solution, which are potentially linked to response to various types of stress.

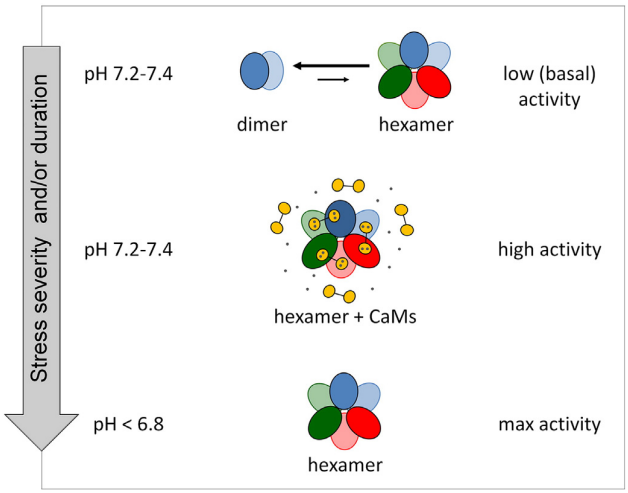

Scheme 1. Biphasic regulation of AtGAD1 oligomerization and activity.

Please cite this article as: A. Astegno, et al., Functional roles of the hexamer organization of plant glutamate decarboxylase, Biochim. Biophys. Acta (2015), http://dx.doi.org/10.1016/j.bbapap.2015.01.001

Acknowledgments

Financial support from the Swiss National Science foundation to GC (grant number 140879) is gratefully acknowledged.

References

[1] D. De Biase, A. Tramonti, F. Bossa, P. Visca, The response to stationary-phase stress conditions in *Escherichia coli*: role and regulation of the glutamic acid decarboxylase system, Mol. Microbiol. 32 (1999) 1198–1211.
[2] J. Bormann, The 'ABC' of GABA receptors, Trends Pharmacol. Sci. 21 (2000) 16–19.
[3] I. Mody, Y. De Koninck, T.S. Otis, I. Soltesz, Bridging the cleft at GABA synapses in the brain, Trends Neurosci. 17 (1994) 517–525.
[4] L.A. Crawford, A.W. Bown, K.E. Breitkreuz, F.C. Guinel, The synthesis of [gamma]-aminobutyric acid in response to treatments reducing cytosolic pH, Plant Physiol. 104 (1994) 865–871.
[5] N. Bouché, A. Fait, D. Bouchez, S.G. Møller, H. Fromm, Mitochondrial succinic-semialdehyde dehydrogenase of the γ-aminobutyrate shunt is required to restrict levels of reactive oxygen intermediates in plants, Proc. Natl. Acad. Sci. 100 (2003) 6843–6848.
[6] A.W. Bown, K.B. MacGregor, B.J. Shelp, Gamma-aminobutyrate: defense against invertebrate pests? Trends Plant Sci. 11 (2006) 424–427.
[7] M.R. Roberts, Does GABA act as a signal in plants? Hints from molecular studies, Plant Signal. Behav. 2 (2007) 408–409.
[8] N. Bouché, B.t. Lacombe, H. Fromm, GABA signaling: a conserved and ubiquitous mechanism, Trends Cell Biol. 13 (2003) 607–610.
[9] R. Palanivelu, L. Brass, A.F. Edlund, D. Preuss, Pollen tube growth and guidance is regulated by POP2, an arabidopsis gene that controls GABA levels, Cell 114 (2003) 47–59.
[10] B.J. Shelp, A.W. Bown, M.D. McLean, Metabolism and functions of gamma-aminobutyric acid, Trends Plant Sci. 4 (1999) 446–452.
[11] W.A. Snedden, T. Arazi, H. Fromm, B.J. Shelp, Calcium/calmodulin activation of soybean glutamate decarboxylase, Plant Physiol. 108 (1995) 543–549.
[12] W.A. Snedden, N. Koutsia, G. Baum, H. Fromm, Activation of a recombinant petunia glutamate decarboxylase by calcium/calmodulin or by a monoclonal antibody which recognizes the calmodulin binding domain, J. Biol. Chem. 271 (1996) 4148–4153.
[13] V.S. Reddy, G.S. Ali, A.S.N. Reddy, Genes encoding calmodulin-binding proteins in the *Arabidopsis* genome, J. Biol. Chem. 277 (2002) 9840–9852.
[14] H. Gut, P. Dominici, S. Pilati, A. Astegno, M.V. Petoukhov, D.I. Svergun, M.G. Grütter, G. Capitani, A common structural basis for pH- and calmodulin-mediated regulation in plant glutamate decarboxylase, J. Mol. Biol. 392 (2009) 334–351.
[15] G. Capitani, D.D. Biase, C. Aurizi, H. Gut, F. Bossa, M.G. Grutter, Crystal structure and functional analysis of *Escherichia coli* glutamate decarboxylase, EMBO J. 22 (2003) 4027–4037.
[16] B. Liao, R.E. Zielinski, Production of recombinant plant calmodulin and its use to detect calmodulin-binding proteins, Methods Cell Biol. 49 (1995) 487–500.
[17] M.M. Bradford, A rapid and sensitive method for the quantitation of microgram quantities of protein utilizing the principle of protein-dye binding, Anal. Biochem. 72 (1976) 248–254.
[18] D.D. Biase, A. Tramonti, R.A. John, F. Bossa, Isolation, overexpression, and biochemical characterization of the two isoforms of glutamic acid decarboxylase from *Escherichia coli*, Protein Expr. Purif. 8 (1996) 430–438.
[19] L.R. Manning, W.T. Jenkins, J.R. Hess, K. Vandegriff, R.M. Winslow, J.M. Manning, Subunit dissociations in natural and recombinant hemoglobins, Protein Sci. 5 (1996) 775–781.
[20] K.A. Ferguson, Starch-gel electrophoresis—application to the classification of pituitary proteins and polypeptides, Metabolism 13 (1964) 985–1002 (Suppl.:).
[21] J.M. Duarte, A. Srebniak, M.A. Scharer, G. Capitani, Protein interface classification by evolutionary analysis, BMC Bioinformatics 13 (2012) 334.
[22] A.J. McCoy, V. Chandana Epa, P.M. Colman, Electrostatic complementarity at protein/protein interfaces, J. Mol. Biol. 268 (1997) 570–584.
[23] J.M. Moulis, V. Davasse, Probing the role of electrostatic forces in the interaction of Clostridium pasteurianum ferredoxin with its redox partners, Biochemistry 34 (1995) 16781–16788.
[24] A.I. Voznesensky, J.B. Schenkman, Quantitative analyses of electrostatic interactions between NADPH-cytochrome P450 reductase and cytochrome P450 enzymes, J. Biol. Chem. 269 (1994) 15724–15731.
[25] H. Gut, E. Pennacchietti, R.A. John, F. Bossa, G. Capitani, D. De Biase, M.G. Grutter, Escherichia coli acid resistance: pH-sensing, activation by chloride and autoinhibition in GadB, EMBO J. 25 (2006) 2643–2651.
[26] B.J. Shelp, G.G. Bozzo, A. Zarei, J.P. Simpson, C.P. Trobacher, W.L. Allan, Strategies and tools for studying the metabolism and function of gamma-aminobutyrate in plants. II. Integrated analysis, Botany-Botanique 90 (2012) 781–793.
[27] H. Knight, M.R. Knight, Abiotic stress signalling pathways: specificity and cross-talk, Trends Plant Sci. 6 (2001) 262–267.
[28] A.M. Kinnersley, F.J. Turano, Gamma aminobutyric acid (GABA) and plant responses to stress, Crit. Rev. Plant Sci. 19 (2000) 479–509.

Please cite this article as: A. Astegno, et al., Functional roles of the hexamer organization of plant glutamate decarboxylase, Biochim. Biophys. Acta (2015), http://dx.doi.org/10.1016/j.bbapap.2015.01.001